

Biochemical analysis of apoptosis to impact of Bacterial Extracellular polymeric substances (EPS) Extract on human breast cancer cell line (MCF-7)

By Iman A Bachay

Biochemical analysis of apoptosis to impact of Bacterial Extracellular polymeric substances (EPS) Extract on human breast cancer cell line (MCF-7)

Iman A. Bachay, Dhamia K. Suker

³⁷ Biology Department /College of Science, University of Basrah, Basrah, Iraq

*Corresponding Author: iman.bachay@uobasrah.edu.iq

ABSTRACT

² Antitumor drug resistance and side effects of antitumor compounds are the most common problems in medicine. Therefore, finding new natural compounds with antitumor activity with low side effects could be interesting. This study was designed ² assay the antitumor activity of the extract from Staphylococcus aureus, against breast cancer, The research was performed as an in vitro study. The effect of the EPS extract on the pr²iferation of MCF-7 cell lines was measured by MTT. Morph⁶¹gical Results of the study showed The most effective antitumor activity has been shown against MCF-7 cell lines comp⁵⁹ to Vero cell lines. The Bcl-2, Bax, p53, caspase3, and caspase9 genes' expression levels in the MCF-7 cells were measured by qPCR, and the results indicated that treating cells with EPS extract significantly increased the expression rate in apoptotic genes. and behavior the MCF-7 cells were driven toward cell death. Based on the results, the bacterial EPS exhibits potential for use as a breast cancer anticancer treatment.

Keywords: EPS, MCF-7 cells, P53, Bax, Caspase3, Casapase9

Introduction

Cancer, a neoplastic disease, an uncontrolled²⁰oliferation of cells results from abnormalities in the cell cycle, which forms tumor tissue and cancer. Breast cancer (BC) is the most common type of cancer and the second leading²³use of cancer-related deaths among women globally [1]. As per the Cancer Statistics 2020 report, An estimated 685,000 women died from breast corresponding to 16% or 1 in every 6 cancer deaths in women [2]. The significant advantages of bacterium-mediated cancer therapy (BMCT) have garnered a lot of interest [3]. For⁶⁸ore than a century, researchers have lo¹²ed into using bacteria as a possible cancer treatment [4]. In patients with bone and soft tissue sarcoma, injection of a preparation of heat-killed Streptococcus pyogenes may cause tumor regression, according to a report originally published by bone surgeon William B. Coley [4]. Thanks to developments in medical technology, BMCT is getting more attention these days [5]. Numerous bacterial species have been investigated, such as Salmonella species, Bifidobacterium, Clostridium, and Streptococcus [6].

Bacterial biofilms are intricate communities of bacteria adhered to surfaces that are kept together by self-produced polymer matrixes known extracellular polymeric substances (EPS) mostly made of

extracellular DNA, secreted proteins, and polysaccharides [7]. They reserve adhesions and prevent desiccation, bacteria release extracellular polymeric compounds into the environment in the form of capsules or slime [8]. Polysaccharides are composed of water-soluble ionic or nonionic polymers [9].

The EPS exhibits effectiveness as an antioxidant, anticancer, and immune-stimulating activity attributes have led to increased attention to EPS as a potential source of novel drugs for cancer, which is regarded as one of the top ten global causes of death. Factors secreted from *S. aureus* biofilms might Impair Immune Response [10].

Studies have shown that genetic backgrounds, such as polymorphisms and gene mutations, play an important role in cancer development [11]. One of the apoptosis pathways is the mitochondria-mediated pathway, which members of the Bcl-2 family of proteins control [12].

B-cell lymphoma 2 The Bcl-2 family includes the antiapoptotic protein Bcl-2 [13]. Depending on how Bcl-2 interacts with other Bcl-2 family members, its function changes [14]. Solid tumors such colon, stomach, ovarian, and breast malignancies express Bcl-2 [15]. Normal mammary tissue expresses Bcl-2 family proteins, such as Bcl-2 and Bax [11]. Bcl-2 is one of the Bcl-2 family members that is directly elevated by estrogen in breast cancer through transcriptional induction [16]. Consequently, BCL2-positive expression in breast cancer is linked to certain outcomes and might be interpreted as an indication of estrogen receptor (ER) activation [17].

Recent studies have suggested that Bcl-2 is a reliable prognostic marker, especially for hormone receptor (HR) positive breast cancer. Also, many studies prove that Bcl-2 is closely related to the occurrence and development of breast cancer by inhibiting cell apoptosis [17]. Currently, the most frequent genetic alteration linked to human neoplasia is the p53 mutation. p53 mutations are linked to more severe disease and a worse overall survival rate [2]. The aim of this study was to investigate the anticancer properties of bacterial EPS extract. Expression of P53, Bcl-2 Bax, caspase-9 and caspase-3 genes in breast cancer cell line (MCF-7).

Materials And Methods

Bacterial strain and Culture medium

The *S. aureus* strains were grown in Tryptic Soy Broth (TSB) was prepared as per the manufacturer's instructions and autoclaved at 121 °C for 15 minutes.

Detection of biofilm formation in Tissue Culture Plate (TCP)

Quantitative biofilm formation on polystyrene biofilm-forming capacity was measured by the determination of adhesion to polystyrene microtiter plates [18].

Development of a mature biofilm of *S. aureus*

Biofilms grown for EPS extraction were prepared by inoculating a glycerol stock of strain (200 µl of *S. aureus*) the (O.D 0.5 at 600 nm), in 400 mL fresh media TSB supplemented with 0.25% to 4% glucose, in 1.5 L Fernbach flasks to provide a larger surface area for biofilm attachment. Biofilms were grown at 37 °C without shaking for 4–5 days until a thick biofilm “sludge” was observed [20].

Extraction crude EPS

Following the establishment of the mature biofilm, the cell pellets were precipitated and disposed of, and the culture broth was centrifuged at 3,500 g for 15 minutes at 4 °C. The supernatant was left overnight at 4 °C with 5% Trichloroacetic acid added to guarantee that all cells were eliminated and that no protein content remained in the supernatant. The supernatant was then centrifuged at 3,500 g. Using 0.1 M NaOH, the pH of the clear supernatant was brought to 7.0. After completing each supernatant to three volumes with 95% ethanol and letting it sit at 4 °C for the night, the precipitate (EPS) was separated by centrifugation at 3,500 g for 20 minutes at 4 °C. It was then twice cleaned with acetone and dehydrated using ether. dried in a desiccator at the end then weighed and stored at room temperature [21].

Structural characterization of the EPS

the dried EPS samples were analyzed by FTIR spectroscopy in attenuated total reflection (ATR) mode using an FTIR spectrometer. The spectrum was recorded in transmittance mode in the range of 400 – 4,000 cm⁻¹ [22].

Preparation of bacterial EPS Extract

bacterial EPS extract was prepared in various quantities by dissolving it in sterile RPMI. Using the filter paper, the resultant solution was filtered twice. Following the sterilization of the solution with 0.22-micron filters, standard stock solution (640 µg/ml) was serially diluted to create concentrations of 20, 80, 160, 320, and 640 µg/ml. [20].

Biological assay

Cell Culture and Treatment

The study effect of bacterial EPS extracts on cell viability was assessed as percent cell viability compared with control on treatment cells, which were arbitrarily assigned 100% viability. Cell lines included, Vero cells as a model for normal cells and MCF-7 a Human breast carcinoma cell lines model cells were purchased from the Pasteur Institute of Iran and maintained in the proper conditions, the cells were maintained and performed as described previously in. The experiments were made up when the cells were in the logarithmic growth phase. This experiment was performed in triplicates and the results were obtained as mean ± SD [23,24].

Cytotoxicity assay

The effect of EPS on the proliferative capacity or viability of the cells was determined using 3-(4,5-dimethylthiazol-2-yl)-2,5-diphenyltetrazolium bromide assay as previously described [23]. This experiment was performed in triplicates and the results were obtained as mean ± SD.

Primers

The forward and reverse primer sequences for RT-PCR and Real-time PCR were selected according to previously published articles, as follows. The primers with reference are shown in (table 1).

Table (1) shows forward and reverse primer sequences

Oligo Name	Primer seq (5-3)	Reference
GAPDH	F 5'-TGAAGGTCGGTGTGAACGGATTTGGTC-3' R 5'-CATGTAGGCCATGAGGTCCACCAC-3'	[25]
Bcl-2	F 5'-ATCTTCTCCTTCCAGCCTGA-3' R 5'-TGCAGCTGACTGGACATCTC-3'	[26]
Bax	F 5'-CTGCAGAGGATGATTGCTGA-3' R 5'-GAGGAAGTCCAGTGTCCAGC-3'	[26]

Caspase 9	F 5'-CGAACTAACAGGCAAGCAG C-3' R 5'-ACCTCACCAAATCCTCCAGAAC-3'	[27]
Caspase 3	F 5'-TGGTTCATCCAGTCGCTTTG-3' R 5'-TGGTTCATCCAGTCGCTTTG-3'	[27]
p53	F 5'-GGCTCTGACTGTACC ACCATCCA-3' R 5'-GGCACAACACGCAC CTCAAAG-3'	[28]

6 RNA Extraction and cDNA Synthesis

RNA extraction and cDNA synthesis was performed as described previously [29].

48 Real-time PCR

Real-time PCR was carried out, table (2.2) contains a list of all primer genes. The expression was calculated by using the relative standard curve method of quantification and reported as a fold change in gene expression [30].

9 Morphological characterization of cell death By Acridine Orange-Ethidium bromide AO/EB

4 Dissolve 1 µg of orange acridine and 1 µg of ethidium bromide with 10 mL of PBS, making the prepared concentration 1%. The dye is prepared under dark conditions and at room temperature. Next, the stain cover slid [31].

6 Statistical Analysis

The data were expressed as mean values ± standard deviation of 39 mean (SD). The difference between control and treated groups was analyzed by One-way ANOVA. A value of P < 0.05 was considered statistically significant.

Result

Study of microbial biofilms by tissue Culture Plate (TCP)

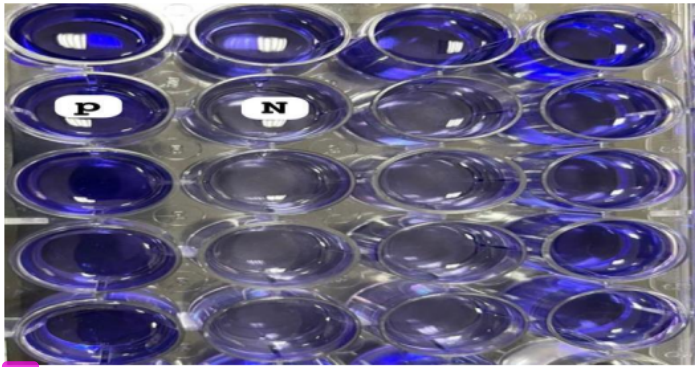
The TCP showed positive results 3 with high significant differences (p< 0.05). The average OD of *S. aureus* was 43 0.310389 ±0. 015 and the average OD of negative control was 0.092167± 0.023. (figure1),(figure 2), (table 2) (table 3).

Table (2) Shows the OD of control samples (A), and (B, C, D) shows the OD of *S. aureus* in micro ELISA

	1	2	3	4	5	6
A	0.06	0.12	0.112	0.097	0.108	0.056
B	0.295	0.263	0.438	0.362	0.489	0.227
C	0.263	0.337	0.525	0.337	0.283	0.219
D	0.293	0.247	0.205	0.272	0.223	0.309

22 * OD of uninoculated medium as (negative control)

22 *OD above that OD considered positive if its OD was twice that of the negative control strain.



14

Figure (1) Screening of biofilm producers by TCP method: high and non-slime producers differentiated with crystal violet staining in 96 well tissue culture plate

EPS of biofilm description

After four days of incubation at 37 °C, Bacteria *S. aureus* displayed a heavy growth on the TSB agar medium and produced opaque, off-white colonies with mucoid texture (figure2). The bacteria *S. aureus* cultured in the stationary phase of development under ideal conditions provided the crude EPS, which were then extracted and purified in accordance with the instructions in (Materials and methods). The figure (3) shows the amounts of the EPS produced by bacteria .

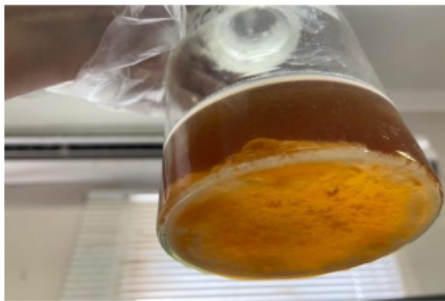


Figure (2) shows heavy growth of biofilm after culture bacteria four days

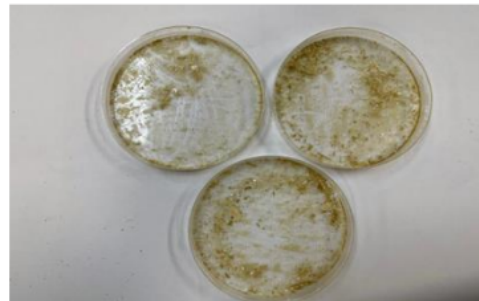


Figure (3) shows the EPS after Extraction steps from biofilm

Characterization of EPS extract

The EPS's FTIR spectrophotometer (table 3) revealed numerous peaks corresponding to the main functional groups of the EPS. The bands between 4000 and 3500 cm^{-1} were identified as the O-H residue's stretching vibrat²¹ in the EPS. The stretching vibration of the lipid (Ch, CH₂, CH₃) appears at the bands at 2800–3000 cm^{-1} . The stretching vibration of the carboxyl group and C=O ap²⁴ in the bands at 1500–1800 cm^{-1} . The EPS's 1500–1800 cm^{-1} bands identified the proteins from the C=O, N–H, and C–N (amideI, amideII) ⁶ idues. The sulfate active group SO₄ is represented at 1800-1000 cm^{-1} , and 900-125 cm^{-1} indicated to Polysaccharides, nucleic acids C-O, C-O-C, N-H (amide III) residue in the EPS (figure 4).

Table (3) Assignments of principal infrared vibrational signals of the (4000-400 cm⁻¹) region of the ART/FT-IR spectrum of the *S. aureus* EPS OF biofilm

Windows of IR spectra corresponding to EPS signals	Principal EPS	Main functional groups in biomolecules
4000-3500 cm ⁻¹	alcoholic group	O-H
3000-3000 cm ⁻¹	lipids	CH,CH ₂ ,CH ₃
1500-1800 cm ⁻¹	Proteins	C=O, N-H, C-N (amide I, amide II)
1800-1000 cm ⁻¹	sulfate	SO ₄
900-125 cm ⁻¹	Polysaccharides, nucleic acids	C-O, C-O-C, N-H (amide III)

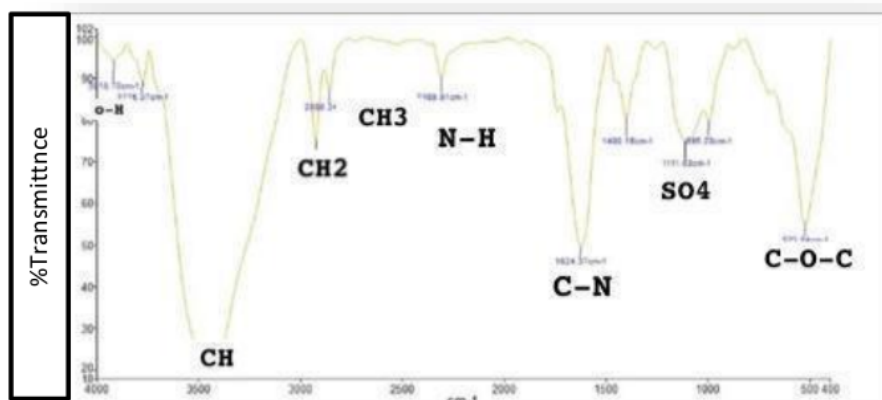


Figure (4) The major functional groups of the EPS that identified using FTIR spectrophotometer Wave number (cm⁻¹) IR Spectrum of EPS from *S. aureus* EPS of biofilm.

Cell viability

When both cells were treated with varying concentrations of EPS extract, the viability and survival rates of the cells decreased considerably in a dose-dependent manner.

Cell viability of impact of *S. aureus* EPS on Vero cell line

Statistically significant difference in the viability of the Vero cell lines' dose-dependent manner were observed in cells treated with EPS. The highest rate of viability Vero cell was at a concentration of 20 µg/ml and the lowest rate of viability was at a concentration of 640 µg/ml. was at different time treatment exposures (24,48,72 h), and there was remarkable inhibition in cell viability represented by a marked inhibitory effect on the cell population also there were no significant differences between viability time-dependent manner, figure (5 A,B), table (4), figure (6).

Table (4) shows cell viability of Vero cells as determined by MTT, after treatment with different concentration of EPS for three times exposure

Concentrations µg/ml	Viability percentage % Vero 24	Viability percentage % Vero 48	Viability percentage % Vero 72
----------------------	-----------------------------------	-----------------------------------	-----------------------------------

0	100±.00	100±.00	100±.00
20	90.95±0.68	90.63±0.56	89.63±0.67
80	86.83±8.44	83.98±8.54	70.99± 8.34
160	79.75±11.80	59.30±10.54	59.30±9.57
320	76.33± 18.81	43.86±17.45	43.87±16.32
640	43.75±0. 46	42.95±0.98	42.95±0.45

7
Values are mean ± SD (n-3)

* Represents a significant difference in comparison between treated groups and control (p<0.05)

Cell viability of impact of EPS on MCF-7 cell lines

31
Statistically significant differences in the viability of the MCF-7 cell lines dose-dependent manner were observed in cells treated with EPS. The highest rate of viability in MCF-7 cells was at a concentration of 20 µg / ml and the lowest rate of viability at a concentration of 640 µg/ml. at different time exposure (24,48,72 h) The IC50 value for Vero was 441.5078µg/ml ,392.8385 µg/ml ,and 323.6588 µg/ml respectively and there was remarkable inhibition in cell viability represented by a marked inhibitory effect on the cell population Also there were no significant differences between the treatments based on time 48 and 72 h, but there was a clear difference between them and time 24h. figure (6), table (5) , and there was remarkable inhibition in cell viability represented by a marked inhibitory effect on the cell population also there were no significant differences between viability time-dependent manner, figure (figure 3.9 A,B), and Compare effect of EPS biofilm on viability between MCF-7 in and Vero cell (figure 3,10,11,11)

Table (5) shows viability percentage of MCF-7cell lines

Concentrations µg/ml	viability percentage % MCF-7 24h	viability percentage % MCF-7 48h	viability percentage % MCF-7 72h
0	100±.00*	100±.00	100±.00
20	84.30±3.561*	89.827±3.651	90.95±2.651
80	61.63±8.97*	75.23±7.88	78.58± 8.44
160	55.86±5.97*	66.89±5.94	62.70±4.97
320	39.45± 9.81*	54.46±7.43	57.914±8.99
640	20.31±1.320*	22.06±1.222	19.48±1.244

29 Assess the half maximal inhibitory concentration (IC₅₀) of EPS

The half maximal inhibitory concentration values were calculated by using the MS Excel curve represented in (Table 6), and the most active dose of EPS that inhibits growth and proliferation of the Vero and MCF-7 cell lines was on 24 h. The IC₅₀ value of Vero cell lines was 479.0123 µg/ml, 454.7238µg/ml ,and 428.9419µg/ml respectively. While The IC₅₀ of MCF-7 cell lines value was 297.4519 µg/ml, 365.8311 µg/ml and 365.8311µg/ml respectively. Also, there was significant difference in IC₅₀ between the time of exposure figure (6).

2 Table(6) Shows comparison of IC₅₀ of Vero and MCF-7 Cell Lines at three time

cell line	IC ₅₀ µg/ml
-----------	------------------------

	Exposure time – 24	Exposure time – 48	Exposure time – 72
Vero	479.0123±.784*	454.7238±1*	428.9419±1*
MCF7	297.4519 ±1*	365.8311±1*	365.2941±1*

Values are mean ± SD (n-3) * Represents a significant difference in comparison between treated groups and control (p<0.05)

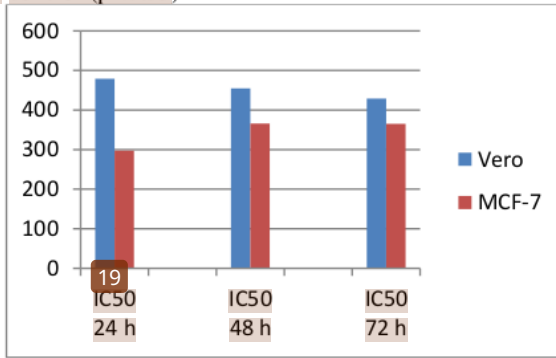


Figure (6) Shows the comparison of IC50 of Vero and MCF-7 Cell Lines at 24,48,72 h

Morphological characterization of cell death by AO/EB for treated cells with EPS

The morphological feature of cell death was also emphasized using fluorescent stain, both MCF-7 and Vero cells were treated with IC50 of EPS. MCF-7 living cells were green with uniform color, early during the initiation of apoptosis, the cells stain green with bright green dots in the nucleus, due to the chromatin condensation and nucleus fragmentation as fig.(7 B,D) shows when compared to untreated control cells it was showed that there was normal morphology and appeared as green uniformly as shown in fig (7A). In the late stage of cell death, the cells stain dense -yellow-green as shown in fig.(7B). However, the Vero cell was treated with the same protocol, and the cells stained green with bright green or yellow-green dotes as shown in fig (7B,D). In contrast, the untreated control group appears as a green uniformly formed as shown in Fig (7A,C).

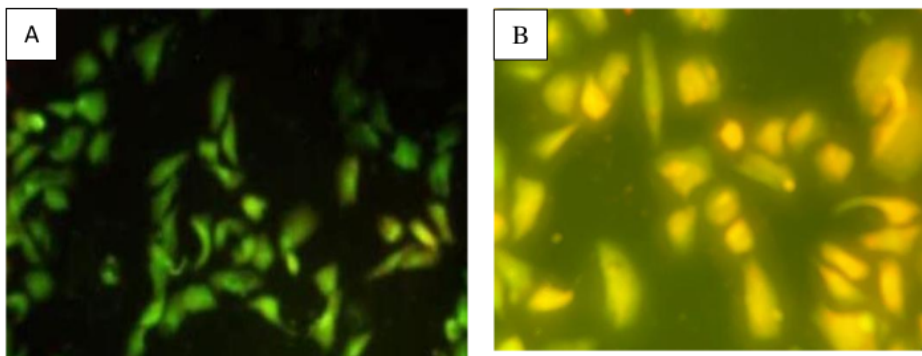


Figure (7) Picture shows treated MCF-7 cells stained with AO/EB. Early apoptotic cells are shown as bright green chromatin that is highly condensed (A10X). Late apoptotic cells have bright orange chromatin that is highly condensed or fragmented (B 40X).

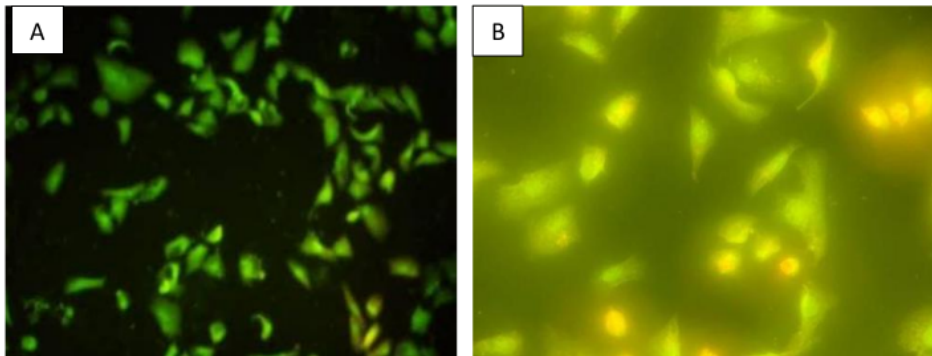


Figure (8) Picture shows treated Vero cells stained with AO/EB. Early apoptotic cells are shown as bright green chromatin that is highly condensed (A10X). Late apoptotic cells have bright orange chromatin that is highly condensed or fragmented (B40X)

Biochemical Analysis of Cell Death by real time PCR

The current study focused on analyzing the genes related to the mitochondrial apoptotic pathway of cellular death following treatment with an IC₅₀ dose of bacterial EPS extract for 48 hours (table 7).

Table (7) shows expression of genes both Vero and LNCaP after treatment with EPS

Group cell line	P53 expression	BAX expression	Bcl-2 expression	Caspase-9 expression	Caspase-3 expression
Vero Treatment with EPS	1.47±.01*	1.23±.01*	1.05±.01*	2.34±.01*	1.47±.01*
MCF-7 Treatment with EPS	1.71±.01	1.45±.01	0.64±.01	3.6±.01	1.47±.01

Values are mean ± SD (n-3) * Represents a significant difference in comparison between treated groups and control (p<0.05)

Induction of Apoptotic in treated MCF-7 by activation P53 gene

According to the results, P53 expression was higher after receiving EPS treatment than its level in the corresponding controls in MCF-7 cell lines. In comparison, Vero's cell lines showed a little increase after the impact of EPS on cell lines (Fig 9).

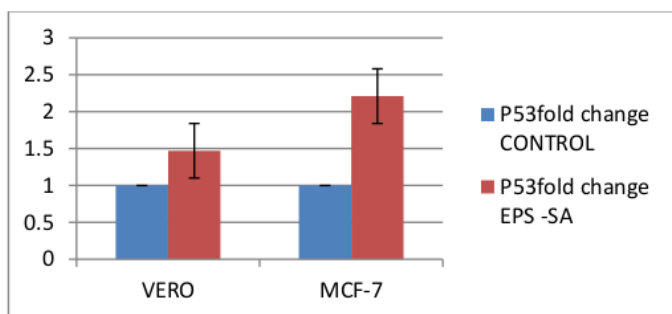


Figure (9) shows graph of relative expression of P53 in Vero and MCF-7 cell treated and untreated with EPS compare to control group.

3.9.2 Induction of Apoptotic in treated MCF-7 by activation of Bax and Bcl-2 genes

Treated human breast cancer cells MCF-7 with EPS resulted in a reduction of Bcl-2 expression with an increase in Bax expression. According to the results, the expression BAX gene in both cell lines relative to the corresponding controls' level expression was shown to have the greatest EPS effect on the Vero and MCF-7 that were treated. (Figure 10) While the result found that the expression of the Bcl-2 gene showed a significant increase ($P < 0.05$) in cancer cell lines MCF-7 compared to its level in the corresponding controls. On the other hand not show any significant decrease in the Vero cell line (Fig 11).

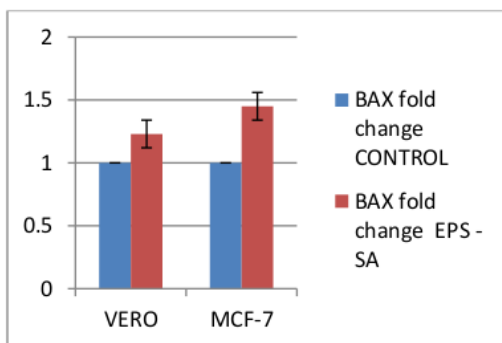


Figure (10) shows graph of BAX relative expression in Vero and MCF-7 cell treated or untreated with EPS compare to control group.

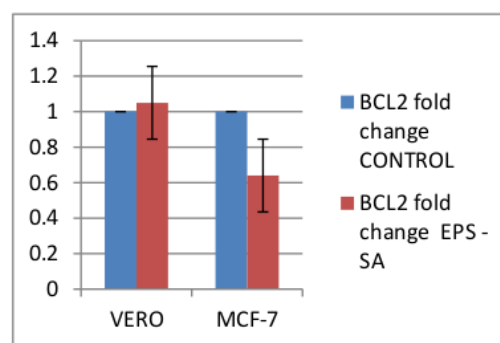


Figure (11) shows graph of relative expression of Bcl-2 in Vero and MCF-7 cell treated and untreated with EPS compare to control group.

Ratio of Bax and Bcl-2 genes

The results demonstrated that in comparison to the control group the 48-hour Bax/Bcl-2 ratio for MCF-7 cells increased considerably at IC50. The table that displays the relative expression changes of the Bax and Bcl-2 genes in the two groups that were treated and controlled is in Figure (12).

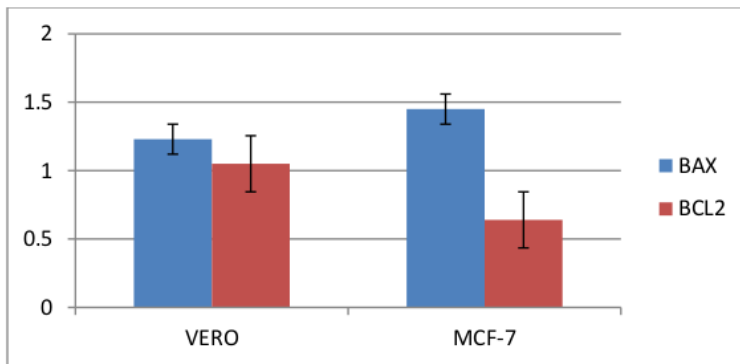


Figure (12) shows graph of ratio of Bax and Bcl-2 in Vero and MCF-7 cell treated and untreated with EPS compare to control group.

Induction of Apoptotic in treated MCF-7 by activation Caspase-3, Caspase-9 genes

The present study shows the expression of caspase-3 significantly increased after being treated with the prepared EPS in human breast cancer cells MCF-7 cell lines compared to the control sample and normal cells (Vero) (Figure 13). Also, treatment leads to activation of the gene Caspase-9 expression in MCF-7 cancer cells treated with EPS at an IC50 dose compared to the control sample and normal cells (Figure 14).

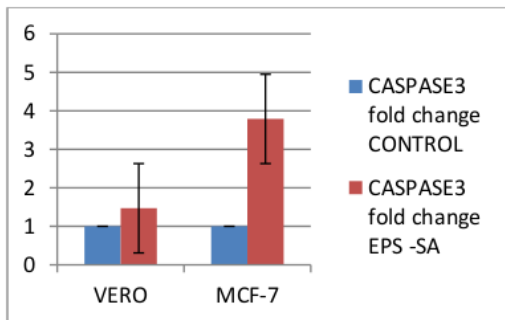


Figure (13) shows graph of relative expression of Caspase-3 in mcf-7and Vero cell treated and untreated with EPS.

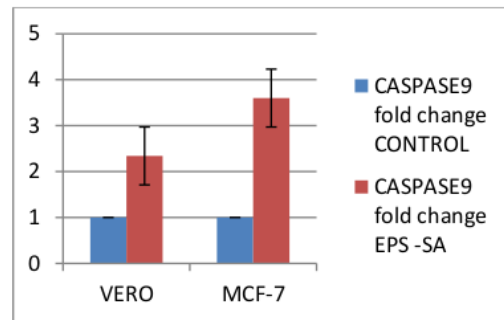


Figure (14) shows graph of relative expression of Caspase-9 in mcf-7and Vero cell treated and untreated with EPS.

Discussion

One of the main causes of the entirely successful in eliminating cancer cells [32]. One of the most promising research directions is using specific types of microorganisms. Because of their many special qualities, they are now seen as a potentially effective platform for cancer therapy [33].

The current investigation aimed to evaluate the cytotoxic effects and antioxidant potential of the extracellular polymer (EPS) biofilm generated by Staphylococcus aureus bacterial strains on MCF-7 cancer cells, and Vero as normal cells. The investigation found that cells treated with EPS experienced a

concentration-dependent decrease in cell viability. And study shows that in cells treated with IC50 values of EPS, the MCF-7 cell lines were shown to be more sensitive to EPS than VERO cell lines and were the most tolerant, this finding demonstrated, the EPS promises regarding potential anti-cancer properties.

32 Nami et al. (2018) observed nearly the same thing: *E. lactis* IW5 secretions had no harmful effects on healthy cells, with 95% of the cells developing normally. Following this context Gasco, Shami, and Crook 2002 found the EPS containing antioxidant efficacy by reestablishing cell redox homeostasis, which prevented the growth of new cells and the development of cancer. According to earlier research (Abdelnasser et al., 2017), *Bacillus megaterium*'s EPS exhibited the highest level of cytotoxicity against HepG2 cells. This significant cytotoxicity was caused by the uronic and sulfuric acids included in the EPS structure. These compounds have cytotoxic and antibacterial properties, making them valuable for usage in biotechnological and medicinal applications. One of these materials is thought to be EPS (Hussain et al., 2017).

Additionally, EPS from *Bacillus* was isolated by Vidhyalakshmi and Vallinachiyar (2013), who found that it was cytotoxic against MCF-7 but not against normal cells. While the majority of EPSs have a relatively constant basic carbohydrate structure, the quantity 31 their substituent groups can vary, altering their activity and characteristics (Wang et al., 2016). In order to investigate the impact of the polymer linkage and substituent functional groups on the biological activity of the polymers, it is usually performed an FTIR to study the EPS extract. In the study of FTIR analysis Wang et al., 2016 findings demonstrated that sulfur was present in the aforementioned EPSs as a substituent functional group.

Because of its qualities, the EPS has drawn more and more interest as a possible source of novel cancer medications. including its efficacy as an antioxidant, anti-cancer, and immune stimulation agent (Mancuso-Nichols et al., 2005). In clinical applications, serious side effects and multidrug resistance have demonstrated the limitations of recent therapeutic techniques. For instance, it has been discovered that polysaccharides produced from MD-b1 exhibit noteworthy therapeutic activity against the endophytic bacteria *Bacillus amyloliquefaciens* which causes stomach 18 cancers (Chen et al., 2013). The anti-proliferation impact of *Lactobacillus casei* 01 EPS on human colon cancer cells, HT-29, rises with dosage, from 5 to 100 µg ml-1. In 27 atological tumor T-cell lines, high sulfated EPS B100S specifically induced significant apoptosis (Liu et al., 2011; Ruiz-Ruiz et al., 2010).

Priyanka et al. (2016) report that a sulfate functional group (2.68%) and 7.08% uronic acid- 65 taining sugars are present in the EPS (650 mg l-1). Because it can bind to the tumor-secreted epidermal growth factor (EGF) and block the Akt 18 3K pathway, this makes it a prospective treatment for brain cancers. This agrees with the finding by Liu et al. (2014) that 13 ionically charged EPS can prevent EGF receptor phosphorylation. The EPS (300g ml-1) showed cytotoxicity against U87MG glioma cells and an IC50 value (234.04 µg ml-1) using the MTT test.

67 From a morphological perspective, apoptosis is characterized as a form of regulated cell death, and it is a crucial cellular route for medical professionals researching and 4 anaging cancer (Wong, 2011). AO/EB fluorescent staining is used to study the morphological changes in Vero and MCF-7 cells as well as the identification of apoptotic signals throughout a 48-hour period at an IC50 concentration of EPS. 9 According to morphological analyses, EPS treated cells exhibited an increase in apoptotic cells when compared to the control group, suggesting that apoptosis may have contributed to the development of the inhibitory action in treated cells. EPS has caused considerable cell detachment from the surface culture, cell shrinkage, and the development of apoptotic bodies in tested cell lines. According to [11] the majority of the contents of the cell are condensed, located on one side of the cell, have bigger cytoplasm, and seem granular. Since their connections weaken, attached cells have a tendency to appear rounder, while loose cells become loose (2017). Condensed nuclei and apoptotic fragments are typical apoptotic features seen in treated cells treated for 72 hours against cancer, according to a study by [11].

Typically, cancer cells develop auto-survival strategies and become resistant to programmed cell death. As a result, apoptosis is a mechanism used by many anticancer drugs to kill tumor cells, making it a desirable target [34]. The current study focused on analyzing the genes related to the mitochondrial apoptotic pathway following treatment with IC50 doses of EPS, evaluating the “in vitro” apoptosis-induced.

According to the current findings, P53 expression increased significantly in response to the treated MCF-7 displayed the highest expression, followed by treated Vero cells. Thus, these findings suggested that EPS enhanced p53 to limit breast cancer cell death. The reason may be due to the p53 plays a controlling gene linked to apoptosis [31,42], and also seems to have a direct effect on mitochondria, potentially encouraging the convergence of extrinsic and intrinsic pathways. It can interact with members of the Bcl2 family to cause apoptosis and mitochondrial outer membrane permeabilization [37,40].

According to our findings, treated MCF-7 that expressed the Bax and Bcl-2 genes had significantly higher ($P < 0.05$) when compared to untreated cells. As a result, malignant cells undergo apoptosis. However, there was no discernible difference between the Vero cell lines that were treated and those that weren't. Because of an increase in the Bax expression ratio on Bcl-2 genes, cancer cells increased cell death. The ratio of Bax to Bcl2 determines if a cell lives or dies. Certain substances have the ability to change the Bax/Bcl-2 ratio, which destroys cancer cells [35]. A study shown the anticancer potential have been change the Bax/Bcl-2 ratio in the AGS cell line and induce the death of malignant cells. Certain compounds found in plants have the ability to raise the Bax/Bcl-2 ratio and kill cancer cells [44]. Many cancer treatment-induced apoptosis is mediated by the activation of tumor protein p53, Bax, and subsequent activation of caspases [35,36].

According to a study by [41], the mitochondrial pathway is involved in EPS-induced apoptosis via up-regulation of Bax and p53 mRNA expression and down-regulation of Bcl-2 mRNA expression. These findings give new information on the potential use of EPS as an anticancer drug in the treatment of human colorectal cancer.

In the current investigation, a significant ($P < 0.05$) rise in the expression of the Bax and Bcl-2 gene at 48 hours of treated MCF-7 cell lines with EPS in contrast to cells that had not received the EPS extract treatment. Consequently, Cancerous cells die as a result of this. However, there was no significant difference between the treated and untreated Vero cell lines.

Cytochrome C is released from the mitochondria and raises the Bax/Bcl-2 expression ratio [13,43]. As a result, caspase activation proteins are produced, which can either be apoptosis effectors (caspases 3, 6, and 7) or initiators (caspases 8, 9, and 10). When caspases are activated, an apoptosome arises. Initiator caspases activate effector caspases, which cause apoptosis by proteolyzing hundreds of proteins [45].

The current study discovered a significant increase in Caspase-9 and Caspase-3 when comparing the treated MCF-7 cell line to the control (untreated cells). These findings imply that EPS may have therapeutic potential in reducing breast tumor progression. However, there was no discernible change between the treated Vero cell lines.

A key component of breast cancer therapy is the stimulation of breast cancer cell apoptosis, which leads to death of breast cancer cells [47]. In apoptotic processes, the activation of the caspases family, particularly caspase-3, is essential. Furthermore, absent caspase-3 in approximately 75% of breast cancer tissues. Therefore highly advised to create a new therapeutic approach and elucidate the process of treating breast cancer via the caspase-3 independent pathway. The effectiveness of therapeutic techniques

to effectively suppress cancer cell proliferation mostly depends on their capacity to induce tumor cell death. The primary mediators of apoptosis activation are effector caspases, which include caspase-3, -6, and -7 [46].

Caspase-9 is the apoptotic initiator protease of the intrinsic or mitochondrial apoptotic pathway, which is triggered at multi-protein activation platforms. Its activation is likely to involve homo-dimerization of the monomeric zymogens. In order to maintain significant catalytic activity, it attaches itself to the apoptosome. According to a different study [35], treating MCF-7 breast cancer cells with the NSAID FR122047 (FR) causes a caspase linear cascade to be activated. They discovered that caspase-9 inhibition may erratically increase cell death [48].

While it is commonly understood that caspase activity is necessary for apoptotic cell death and that certain caspase inhibitors may block this process, new research indicates that caspase inhibitors can also stimulate necrotic cell death and even improve stress-induced apoptosis [49] [14], and [15]. It is still necessary to conduct a thorough examination of caspase functions that goes beyond the conclusions of earlier research [49].

Conclusion

Staphylococcus aureus EPS extract has IC50 values on cancer cells, the EPS extract shows a promising effect on cancer cells for use as an anticancer. The extract-induced apoptosis is mediated by the activation of tumor proteins p53, Bax, Bcl2, and caspases, and induction of the MCF-7, these anticancer properties are proved by qPCR for apoptotic genes. The interesting outcomes of our study have revealed the possibility of the EPS induction program cell death that led to the cell death of MCF-7.

Reference

- [1] M. Parton, M. Dowsett, and I. Smith, "Studies of apoptosis in breast cancer," *Bmj*, vol. 322, no. 7301, pp. 1528–1532, 2001.
- [2] M. Gasco, S. Shami, and T. Crook, "The p53 pathway in breast cancer," *Breast cancer Res.*, vol. 4, pp. 1–7, 2002.
- [3] P. Sarotra and B. Medhi, "Use of bacteria in cancer therapy," *Curr. Strateg. Cancer Gene Ther.*, pp. 111–121, 2016.
- [4] F. Badie *et al.*, "Use of Salmonella bacteria in cancer therapy: direct, drug delivery and combination approaches," *Front. Oncol.*, vol. 11, p. 624759, 2021.
- [5] M. T.-Q. Duong, Y. Qin, S.-H. You, and J.-J. Min, "Bacteria-cancer interactions: bacteria-based cancer therapy," *Exp. Mol. Med.*, vol. 51, no. 12, pp. 1–15, 2019.
- [6] D. L. Mager, "Bacteria and cancer: cause, coincidence or cure? A review," *J. Transl. Med.*, vol. 4, no. 1, pp. 1–18, 2006.
- [7] T. A. Alboslemy, *Kruppel-like factor 2: A regulator of macrophage-mediated innate immune response against Staphylococcus aureus biofilm*. Kent State University, 2018.
- [8] I. Wijesekara, R. Pangestuti, and S.-K. Kim, "Biological activities and potential health benefits of sulfated polysaccharides derived from marine algae," *Carbohydr. Polym.*, vol. 84, no. 1, pp. 14–21, 2011.
- [9] C. A. V Torres *et al.*, "Kinetics of production and characterization of the fucose-containing exopolysaccharide from Enterobacter A47," *J. Biotechnol.*, vol. 156, no. 4, pp. 261–267, 2011.

- [10] T. Alboslemy, B. Yu, T. Rogers, and M.-H. Kim, "Staphylococcus aureus biofilm-conditioned medium impairs macrophage-mediated antibiofilm immune response by upregulating KLF2 expression," *Infect. Immun.*, vol. 87, no. 4, pp. e00643-18, 2019.
- [11] M. H. Sangour and S. By, "Gene expression profile of apoptotic genes following exposure of mammalian cell lines to nanoparticles (in-vitro study)," 2020.
- [12] C. F. A. Warren, M. W. Wong-Brown, and N. A. Bowden, "BCL-2 family isoforms in apoptosis and cancer," *Cell Death Dis.*, vol. 10, no. 3, p. 177, 2019.
- [13] S. Qian, Z. Wei, W. Yang, J. Huang, Y. Yang, and J. Wang, "The role of BCL-2 family proteins in regulating apoptosis and cancer therapy," *Front. Oncol.*, vol. 12, p. 985363, 2022.
- [14] A. Basu, "The interplay between apoptosis and cellular senescence: Bcl-2 family proteins as targets for cancer therapy," *Pharmacol. Ther.*, vol. 230, p. 107943, 2022.
- [15] R. Singh, A. Letai, and K. Sarosiek, "Regulation of apoptosis in health and disease: the balancing act of BCL-2 family proteins," *Nat. Rev. Mol. cell Biol.*, vol. 20, no. 3, pp. 175–193, 2019.
- [16] N. Kunac, N. Filipović, S. Kostić, and K. Vukojević, "The Expression Pattern of Bcl-2 and Bax in the Tumor and Stromal Cells in Colorectal Carcinoma," *Med.*, vol. 58, no. 8, 2022, doi: 10.3390/medicina58081135.
- [17] L. Clusan, F. Ferrière, G. Flouriot, and F. Pakdel, "A Basic Review on Estrogen Receptor Signaling Pathways in Breast Cancer," *Int. J. Mol. Sci.*, vol. 24, no. 7, p. 6834, 2023.
- [18] N. Malik, D. Bisht, J. Aggarwal, and A. Rawat, "Phenotypic Detection of Biofilm Formation in Clinical Isolates of Methicillin-Resistant Staphylococcus aureus," *Asian J. Pharm. Res. Heal. Care*, vol. 14, no. 1, p. 43, 2022.
- [19] A. Hassan, J. Usman, F. Kaleem, M. Omair, A. Khalid, and M. Iqbal, "Evaluation of different detection methods of biofilm formation in the clinical isolates," *Brazilian J. Infect. Dis.*, vol. 15, no. 4, pp. 305–311, Jul. 2011, doi: 10.1590/S1413-86702011000400002.
- [20] P. M. Bales, E. M. Renke, S. L. May, Y. Shen, and D. C. Nelson, "Purification and characterization of biofilm-associated EPS exopolysaccharides from ESKAPE organisms and other pathogens," *PLoS One*, vol. 8, no. 6, p. e67950, 2013.
- [21] S. M. Abdelnasser *et al.*, "Antitumor exopolysaccharides derived from novel marine bacillus: isolation, characterization aspect and biological activity," *Asian Pacific J. Cancer Prev. APJCP*, vol. 18, no. 7, p. 1847, 2017.
- [22] Z. U. Rehman, J. S. Vrouwenvelder, and P. E. Saikaly, "Physicochemical properties of extracellular polymeric substances produced by three bacterial isolates from biofouled reverse osmosis membranes," *Front. Microbiol.*, vol. 12, p. 668761, 2021.
- [23] R. I. Freshney, *Culture of animal cells: a manual of basic technique and specialized applications*. John Wiley & Sons, 2015.
- [24] Z. A. Mazyed, D. K. Suker, and A. T. Tawfeeq, "ANTIOXIDANT, ANTI-TUMOR ACTIVITY OF CICHORIUM INTYBUS EXTRACTS ON TWO CELL LINES IN VITRO.," *Biochem. Cell. Arch.*, vol. 21, no. 2, 2021.
- [25] M. Bosso and F. Al-Mulla, "RKIP & GSK3 β : The interaction of two intracellular signaling network

regulators and their role in cancer,” in *Prognostic and Therapeutic Applications of RKIP in Cancer*, Elsevier, 2020, pp. 147–173.

- [26] C. Xiong *et al.*, “Induction of apoptosis in HeLa cells by a novel peptide from fruiting bodies of *morchella importuna* via the mitochondrial apoptotic pathway,” *Evidence-Based Complement. Altern. Med.*, vol. 2021, 2021.
- [27] W. Yaoxian, Y. Hui, Z. Yunyan, L. Yanqin, G. Xin, and W. Xiaoke, “Emodin induces apoptosis of human cervical cancer hela cells via intrinsic mitochondrial and extrinsic death receptor pathway,” *Cancer Cell Int.*, vol. 13, no. 1, pp. 1–8, 2013.
- [28] Y. Zhang *et al.*, “CDS-1548 induces apoptosis in HeLa cells by activating caspase 3,” *Oncol. Lett.*, vol. 18, no. 2, pp. 1881–1887, 2019.
- [29] T. Mitupatum *et al.*, “Hep88 mAb-mediated paraptosis-like apoptosis in HepG2 cells via downstream upregulation and activation of caspase-3, caspase-8 and caspase-9,” *Asian Pacific J. Cancer Prev.*, vol. 16, no. 5, pp. 1771–1779, 2015.
- [30] K. J. Livak and T. D. Schmittgen, “Analysis of relative gene expression data using real-time quantitative PCR and the $2^{-\Delta\Delta C_T}$ normalized to glyceraldehyde-3-phosphate dehydrogenase levels. qRT-PCR was method,” *methods*, vol. 25, pp. 402–408, 2001.
- [31] M. H. Sangour, I. M. Ali, Z. W. Atwan, and A. A. A. L. A. Al Ali, “Effect of Ag nanoparticles on viability of MCF-7 and Vero cell lines and gene expression of apoptotic genes,” *Egypt. J. Med. Hum. Genet.*, vol. 22, pp. 1–11, 2021.
- [32] M. T. Amjad, A. Chidharla, and A. Kasi, “Cancer chemotherapy,” 2020.
- [33] Z. Kahrarian, M. Horriat, and S. Khazayel, “A Review of Novel Methods of the Treatment of Cancer by Bacteria,” vol. 1, no. 1, pp. 25–36, 2019.
- [34] B. A. Carneiro and W. S. El-Deiry, “Targeting apoptosis in cancer therapy,” *Nat. Rev. Clin. Oncol.*, vol. 17, no. 7, pp. 395–417, 2020.
- [35] D. Korbakis and A. Scorilas, “Quantitative expression analysis of the apoptosis-related genes BCL2, BAX and BCL2L12 in gastric adenocarcinoma cells following treatment with the anticancer drugs cisplatin, etoposide and taxol,” *Tumor Biol.*, vol. 33, no. 3, pp. 865–875, 2012.
- [36] F. Chen, W. Wang, and W. S. El-Deiry, “Current strategies to target p53 in cancer,” *Biochem. Pharmacol.*, vol. 80, no. 5, pp. 724–730, 2010.
- [37] C. Stolz *et al.*, “Targeting Bcl-2 family proteins modulates the sensitivity of B-cell lymphoma to rituximab-induced apoptosis,” *Blood, J. Am. Soc. Hematol.*, vol. 112, no. 8, pp. 3312–3321, 2008.
- [38] F. B. Furnari *et al.*, “Malignant astrocytic glioma: genetics, biology, and paths to treatment,” *Genes Dev.*, vol. 21, no. 21, pp. 2683–2710, 2007.
- [39] L. D. Attardi and T. Jacks, “The role of p53 in tumour suppression: lessons from mouse models,” *Cell. Mol. Life Sci. C.*, vol. 55, pp. 48–63, 1999.
- [40] N. Rivlin, R. Brosh, M. Oren, and V. Rotter, “Mutations in the p53 tumor suppressor gene: important milestones at the various steps of tumorigenesis,” *Genes Cancer*, vol. 2, no. 4, pp. 466–474, 2011.
- [41] N. Li *et al.*, “Advances in dietary polysaccharides as anticancer agents: Structure-activity relationship,”

Trends Food Sci. Technol., vol. 111, pp. 360–377, 2021.

- [42] M. Ahamed, H. A. Alhadlaq, M. A. M. Khan, and M. J. Akhtar, “Selective killing of cancer cells by iron oxide nanoparticles mediated through reactive oxygen species via p53 pathway,” *J. nanoparticle Res.*, vol. 15, pp. 1–11, 2013.
- [43] A. Boice and L. Bouchier-Hayes, “Targeting apoptotic caspases in cancer,” *Biochim. Biophys. Acta (BBA)-Molecular Cell Res.*, vol. 1867, no. 6, p. 118688, 2020.
- [44] N. Kazemi and S. B. Shahrestani, “Effect of saffron extract on expression of Bax and Bcl-2 genes in gastric adenocarcinoma cell line (AGS),” *Gene, Cell Tissue*, vol. 5, no. 3, 2018.
- [45] D. W. Nicholson, “Caspase structure, proteolytic substrates, and function during apoptotic cell death,” *Cell Death Differ.*, vol. 6, no. 11, pp. 1028–1042, 1999.
- [46] H. C. Chang, S. T. Chen, S. Y. Chien, S. J. Kuo, H. T. Tsai, and D. R. Chen, “Capsaicin may induce breast cancer cell death through apoptosis-inducing factor involving mitochondrial dysfunction,” *Hum. Exp. Toxicol.*, vol. 30, no. 10, pp. 1657–1665, 2011.
- [47] P. Li *et al.*, “Caspase-9: structure, mechanisms and clinical application,” *Oncotarget*, vol. 8, no. 14, p. 23996, 2017.
- [48] H.-S. Jeong *et al.*, “Involvement of caspase-9 in autophagy-mediated cell survival pathway,” *Biochim. Biophys. Acta (BBA)-Molecular Cell Res.*, vol. 1813, no. 1, pp. 80–90, 2011.
- [49] A. A. Ameen and D. K. Suker, “MIR30a suppresses prostate cancer cells by increasing apoptosis and regulation of MMPs,” *Eurasian Med. Res. Period.*, vol. 9, pp. 26–34, 2022.